



Cite this: *RSC Adv.*, 2020, **10**, 12695

Received 4th March 2020
 Accepted 23rd March 2020

DOI: 10.1039/d0ra02055a
rsc.li/rsc-advances

Organic halides, such as chloroform,^{1–5} dioxin,⁶ and iodo-methane⁷ critically influence biological systems and the environment. In the case of chloroform, inhalation of the vapor can cause cancer. Therefore, for decontamination purposes, halogenated compounds need to be detected, no matter how low the concentration. Existing halogenated compounds have generally been determined using gas chromatography.⁸ In addition, liquid chromatography is a useful method for separating these compounds from pollutants.⁹ However, these methods require pollutant samples to be processed by gel-permeation chromatography and/or silica-gel column chromatography, which can be arduous. Hence, new methodology for the detection of organic halides is required.

Recently, chromism has attracted significant attention and has been used to understand a variety of conditions and to engineer products. Numerous types of chromic behavior exist, such as photochromism,¹⁰ mechanochromism,^{11,12} electrochromism,¹³ piezochromism,¹⁴ vapochromism,^{15–17} and solvatochromism.^{18–20} Colors emerging from most forms of chromism are caused by the metamorphoses of compounds with conjugated donor and acceptor units. 1,2-Dithienylethene, which turns red when irradiated with ultraviolet (UV) light, is a famous photochromic material reported by Irie and coworkers.^{21–23} The intramolecular conjugation length of this compound increases by a ring-closing photoreaction. Solvatochromism in solvents of different polarity is due to a variation in its absorption or emission spectrum in each solvent. Because organic halide solvents are of low polarity, they can be used to investigate new methods for detecting organic halides

Halogen-sensitive solvatochromism based on a phenolic polymer of tetraphenylethene†

Takahiro Kakuta, ^a^{ab} Ryota Nakanishi,^a Tomoki Ogoshi^{bc} and Tada-aki Yamagishi^{a*}

Herein, we describe the successful preparation of a methylene-bonded tetraphenylethene polymer using a phenolic-resin synthesis protocol. Our novel phenolic polymer showed solvatochromism in response to halogenated organic solvents. Solvatochromism is induced by halogen/π interactions between the polymer and the organic halide.

because a color transition can occur without an external stimulus, such as light and heat. Previously, yellow-to-red solvatochromism through intramolecular charge transfer in halogenated solvents has been achieved.^{24–26}

The chemical structures of the donor and acceptor units are important when designing and preparing solvatochromic materials. However, it is often difficult to prepare and control the solubilities of these compounds. In addition, crystallinity is an important factor for single-molecule solvatochromism. From these viewpoints, polymer structures are attractive platforms for inducing chromic properties because the solubility of the polymer and its binding sites for organic halides can be controlled. In this study, a novel polymer constructed using 1,1,2,2-tetra(4-methoxyphenyl)ethene (TPE-4MeO) and methylene linkers was prepared by phenolic-polymer synthesis. Phenolic polymers are a class of artificial polymer prepared from phenols and formaldehyde.²⁷ Their high mechanical strengths and chemical and thermal stabilities make these products useful for engineering plastics. Our novel phenolic polymer showed solvatochromism in response to halogenated organic solvents through color changes; in addition, it showed guest and halide selectivity.

The phenolic polymer was constructed from TPE units bonded through methylene linkers, and was synthesized according to a previously reported procedure.²⁸ The TPE-based phenolic polymer (TPE-P) was synthesized by polymerizing TPE-4MeO and paraformaldehyde with sulfuric acid in a mixed solution of acetic acid and chloroform (Fig. 1a). The ¹H NMR spectrum exhibited peak broadening with increasing molecular weight, and the ¹³C NMR spectrum exhibited a signal for a methylene unit after polymerization (Fig. S1–S3†). GPC (Fig. S4†) and MALDI-ToF-MS of TPE-P revealed: $M_n = 1.3 \times 10^3$, $M_w = 2.7 \times 10^3$, $D = 2.1$. Other branching and molecular weights polymers could not be obtained using other substituted TPE monomers, which had its reactive positions blocked by methylene (Fig. S5–S7†). In addition, a single ¹³C NMR methylene peak was observed, which suggests that TPE-P is composed of a single, linear polymer structure.

^aGraduate School of Natural Science and Technology, Kanazawa University, Kakuma-machi, Kanazawa 920-1192, Japan. E-mail: kakuta@se.kanazawa-u.ac.jp; yamagisi@se.kanazawa-u.ac.jp

^bWPI Nano Life Science Institute (WPI-NanoLSI), Kanazawa University, Kakuma-machi, Kanazawa 920-1192, Japan

^cGraduate School of Engineering, Kyoto University, Katsura, Nishikyo-ku, Kyoto, 615-8510, Japan

† Electronic supplementary information (ESI) available. See DOI: 10.1039/d0ra02055a





Fig. 1 (a) Synthesis of TPE-P from TPE-4MeO and paraformaldehyde. (b) Photographic images of solvatochromism in various solvents.

The solubilities of TPE-P (40 g L^{-1}) were investigated in chloroform (CHCl_3), dichloromethane (CH_2Cl_2), tetrahydrofuran (THF), and dimethyl sulfoxide (DMSO) (Fig. 1b). TPE-P in the halogenated and non-halogenated solvents exhibited different colors; the former were red but the latter were yellow. Fig. 2a shows the UV-Vis spectra of each TPE-P solution. Although 510 nm absorption peaks were observed in the spectra of TPE-P in the halogenated solvents, such peaks were absent in the spectra in the non-halogen solvents. The observed color generally corresponds to the wavelength of the complementary visible color, as given by the color circle. In addition, the concentration of the visible color is related to the absorption intensity. The halogenated-solvent solutions were red because the 510 nm absorption wavelength is complementary to red. The CH_2Cl_2 solution absorbed more strongly than the CHCl_3 , THF + HCl, and THF solutions. Similarly, the color concentration of the CH_2Cl_2 solution was higher. To investigate the effects of halogenated compounds on solvatochromism, $1.1 \times 10^{-5} \text{ mol HCl}$ was added to the solution of TPE-P in THF (Fig. 2a, purple spectrum); this mixture was also red and exhibited a similar absorption peak at 510 nm. Because other halogenated compounds such as carbon tetrachloride, bromoform and bromoethane were also exhibited red, these results suggest that yellow-to-red solvatochromism is induced by halogenated compounds.

As we speculated that the solvatochromism behavior of TPE-P requires interaction with a halogenated compound, we next investigated the interactions between halogenated compounds and TPE-P by ^1H NMR spectroscopy. Fig. 2b shows the ^1H NMR spectra of TPE-P in various deuterated solvents. NMR peaks corresponding to aromatic and alkoxy groups were observed in both non-halogenated and halogenated solvents; however, the chemical shifts of these peaks were downfield-shifted only in the halogenated solvents. These downfield shifts are due to lower electron densities in these compounds; hence, these shifts indicate that halogenated compounds and TPE-P interact through halogen/ π interactions, which are non-covalent bonds previously reported in computational studies.^{29–31} Electrostatic and dispersion energies were reported to be the main

contributors to halogen/ π interactions between aromatic compounds and halogen atoms. As a result of these halogen/ π interactions, TPE-P exhibits solvatochromism through changes in its ground state that results from conformational changes to the polymer structure in the presence of an organic halide. In addition, halogen/ π interactions are achieved in aromatic compounds bearing halogen atoms in which the halogen atom binds to the same halogen or carbon. With this in mind, we investigated the solution states by FT-IR spectroscopy, the results of which are shown in Fig. 2c. The IR spectrum of TPE-P shows C–O stretching vibrations at 1250 cm^{-1} and 1050 cm^{-1} . Both vibrational peaks dramatically shift in dichloromethane and chloroform compared to the non-halogenated solvents. The asymmetric stretching peak at 1250 cm^{-1} separates into two peaks, and the symmetric stretching peak at 1050 cm^{-1} shifts to a lower wavenumber. A shift to a lower wavenumber is generally associated with a decrease in electron density. Therefore, the symmetric stretching peak at 1050 cm^{-1} was low-shifted through interactions with halogenated compounds. Similarly,

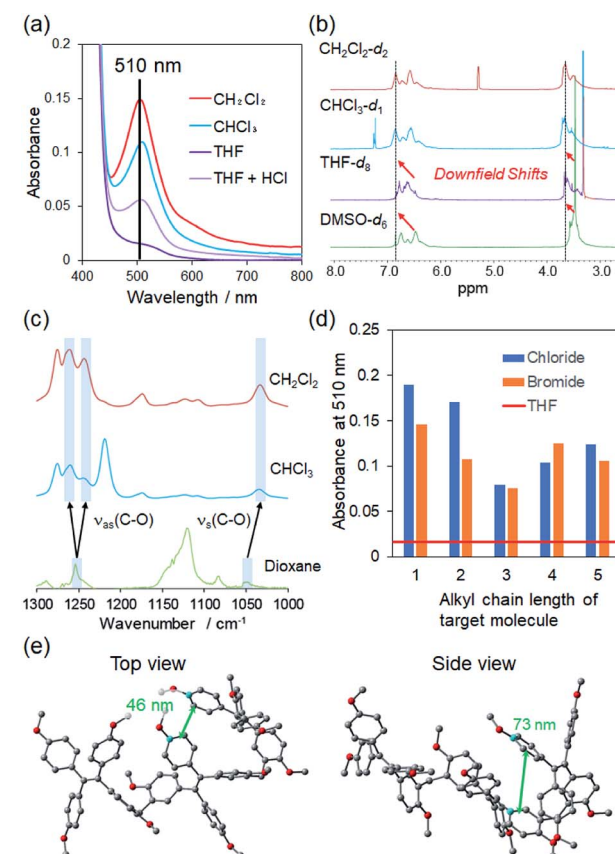


Fig. 2 (a) UV-Vis absorption spectra of TPE-P in various solvents; 510 nm is the complementary wavelength of visible red. (b) ^1H NMR spectra in various deuterated solvents. The aromatic peak is downfield-shifted in halogenated solvents compared to non-halogenated solvents. (c) FT-IR spectra of TPE-P in CHCl_3 and CH_2Cl_2 . (d) UV-Vis absorbance at 510 nm as a function of the chain length of the alkyl halide. (e) DFT ground-state optimized structure of a model TPE-P trimer calculated by B3LYP/3-21G showing the distances between aromatic units, which provide good fits for 1,2-DCE and 1,4-DCB.



the asymmetric stretching peak at 1250 cm^{-1} was also affected by halogenated compounds.

In addition, 2D NOESY NMR spectroscopy showed a correlation peak between TPE-P and 1,2-dichloroethane (Fig. S8†), which indicates that TPE-P solvatochromism is induced through halogen/ π interaction with halogenated compounds. On the other hand, we evaluated the effects of free anions as the solvatochromism targets (Fig. S9†). Various anions, including chloride, bromide, tetrafluoroborate, hypochlorite, and hexafluorophosphate, were dissolved with TPE-P in 1,4-dioxane. These solutions were yellow and did not show any color change. The relationships between dielectric constant, E_T (30), of organic halides and UV-vis absorption maxima were also investigated in Fig. S14.† Every point was appeared at different wavelength and absorption without systematically lined up. The number of organic halides in TPE-P was different in THF solution because our solvatochromism had dependency on molecular size of organic halides. Moreover, TPE-4MeO did not show any solvent dependency, which indicates that TPE-P can selectively detect organic halides solvatochromatically through halogen/ π interactions.

To investigate the solvatochromism mechanism, other organic halides were examined by UV-Vis absorption spectroscopy (Fig. S10†). TPE-P was dissolved in 1,2-dichloroethane (1,2-DCE), 1,3-dichloropropane (1,3-DCP), 1,4-dichlorobutane (1,4-DCB), and 1,5-dichloropentane (1,5-DCP). Not only did the dichloromethane solution exhibit solvatochromism, but the other halogenated solutions did so too. The absorbances of the various halogenated compounds were compared (Fig. 2d); the 510 nm absorption in 1,3-DCP was weaker than in the other halogenated solvents. Similar trends were observed when dibromoalkanes were used as alternative halogenated compounds (Fig. S11†), which suggests that the halogen/ π interactions are influenced by the size of the halogen and/or the compound. To compare the effect of the halogen, we determined the binding constants of 1,2-DCE and 1,2-dibromoethane (1,2-DBE) with TPE-P using Hill's plots (Fig. S12 and S13†). The binding constant (K_a) of 1,2-DCE was found to be $1.4 \times 10^1\text{ M}^{-1}$, while that of 1,2-DBE was determined to be $7.1 \times 10^0\text{ M}^{-1}$; *i.e.*, K_a for 1,2-DCE is 10-times higher than that of 1,2-DCB. Because halogen/ π interactions strongly depend on electronegativity, the chloride in 1,2-DCE interacts more strongly with TPE-P.

We next determined the distances between TPE-P units by optimizing the geometry of a model trimer by DFT at B3LYP/3-21G. Distances of 46 nm and 73 nm were determined between the aromatic units of TPE-P (Fig. 2e); 1,2-DCE and 1,4-DCB fit well into the spaces created by these distances, respectively. On the other hand, there is insufficient space to accommodate 1,3-DCP. These computational results were confirmed by absorption-intensity data, as shown in Fig. 2d. Halogenated compounds with sizes similar to the above-mentioned distances exhibit higher absorption intensities than compounds of other size. These results indicate that TPE-P shows solvatochromism by interacting with halogen compounds at the unit-molecule level.

Finally, we investigated the ability of TPE-P to detect aromatic halides (Fig. 3a). TPE-P solutions in chlorobenzene

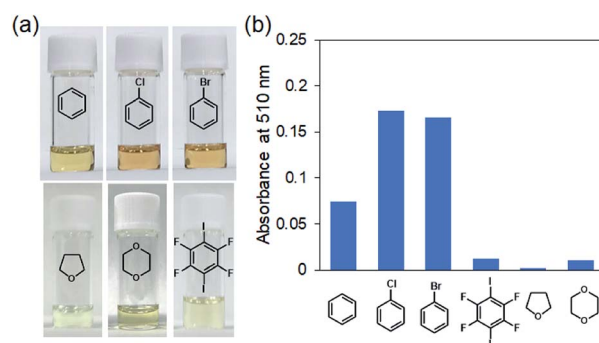


Fig. 3 (a) Photographic images of TPE-P solutions in aromatic compounds and (b) effect of aromatic compounds on absorbance. Aromatic compounds exhibited solvatochromism.

and bromobenzene were red; this color was also produced using benzene as the solvent, which indicates that this solvatochromism occurs through interactions between TPE-P and the aromatic compounds. Although the benzene solution absorbed less than the other aromatic halides, it nevertheless exhibited solvatochromism (Fig. 3b). In contrast, the 1,4-diiodobenzene solution was yellow and absorbed poorly, despite being halogenated because the concentration was low due to low solubility in THF. Clearly, dihaloalkane solvatochromatic behavior depends on molecular size, which indicates that TPE-P requires a guest compound with interaction sites and a molecular size matched to its available space to exhibit solvatochromism.

In conclusion, we successfully prepared a methylene linked tetraphenylethene polymer by phenolic-resin synthesis. The polymer showed solvatochromism and turned red in solutions of halogenated compounds. Experiments with various alkyl halides and DFT calculations at B3LYP/3-21G reveal that halogen/ π and π - π interactions between aromatic and halogenated compound induce this phenomenon. Although the polymer was bonded through methylene linkers and was not conjugated, solvatochromism occurs through interactions with guest molecules. Our results suggest that this phenolic polymer may be applied in industrial fields as a sensing, biological, or aerospace material.

Conflicts of interest

There are no conflicts to declare.

Acknowledgements

This work was supported by World Premier International Research Center Initiative (WPI), MEXT, Japan.

References

- 1 N. Sridhar, C. Krishnakishore, Y. Sandeep, P. Sriramnaveen, Y. Manjusha and V. Sivakumar, *Renal Failure*, 2011, **33**, 1037–1039.
- 2 S. H. Choi, S. W. Lee, Y. S. Hong, S. J. Kim, S. W. Moon and J. D. Moon, *Emerg. Med. J.*, 2006, **23**, 394–395.



3 B. F. Hwang, J. J. Jaakkola and H. R. Guo, *Environ. Health*, 2008, **7**, 23.

4 T. A. Krasnova, I. V. Timoshchuk, A. K. Gorelkina and O. V. Belyaeva, *Foods Raw Mater.*, 2018, **6**, 230–241.

5 H. Kim, *Am. J. Emerg. Med.*, 2008, **26**, 1073.e3–1073.e6.

6 S. S. White and L. S. Birnbaum, *J. Environ. Sci. Health, Part C: Environ. Carcinog. Ecotoxicol. Rev.*, 2009, **27**, 197–211.

7 C. R. Kirman, L. M. Sweeney, M. L. Gargas and J. H. Kinzell, *Inhalation Toxicol.*, 2009, **21**, 537–551.

8 S. D. Richardson, *Anal. Chem.*, 2004, **76**, 3337–3364.

9 K. Haraguchi, Y. Kato, K. Atobe, S. Okada, T. Endo, F. Matsubara and T. Oguma, *Anal. Chem.*, 2008, **80**, 9748–9755.

10 O. S. Bushuyev and C. J. Barrett, in *Photomechanical Materials, Composites, and Systems*, ed. T. J. White, John Wiley & Sons, Hoboken, 2017, pp. 37–77.

11 A. Lavrenova, D. W. Balkenende, Y. Sagara, S. Schrett, Y. C. Simon and C. Weder, *J. Am. Chem. Soc.*, 2017, **139**, 4302–4305.

12 S. A. Sharber, K. C. Shih, A. Mann, F. Frausto, T. E. Haas, M. P. Nieh and S. W. Thomas, *Chem. Sci.*, 2018, **9**, 5415–5426.

13 S. H. Hsiao, W. K. Liao and G. S. Liou, *Polymers*, 2017, **9**, 511.

14 Y. Cao, L. Lewis, W. Y. Hamad and M. J. MacLachlan, *Adv. Mater.*, 2019, **31**, e1808186.

15 T. Ogoshi, Y. Shimada, Y. Sakata, S. Akine and T. A. Yamagishi, *J. Am. Chem. Soc.*, 2017, **139**, 5664–5667.

16 S. Colodrero, M. Ocaña, A. R. González-Elipe and H. Míguez, *Langmuir*, 2008, **24**, 9135–9139.

17 T. Tsukamoto, R. Aoki, R. Sakamoto, R. Toyoda, M. Shimada, Y. Hattori, Y. Kitagawa, E. Nishibori, M. Nakano and H. Nishihara, *Chem. Commun.*, 2017, **53**, 9805–9808.

18 H. Naito, K. Nishino, Y. Morisaki, K. Tanaka and Y. Chujo, *Angew. Chem., Int. Ed.*, 2017, **56**, 254–259.

19 J. Qu, W. Liao, H. Chen and T. Masuda, *Macromol. Biosci.*, 2009, **9**, 563–567.

20 J. Bouchard, M. Belletête, G. Durocher and M. Leclerc, *Macromolecules*, 2003, **36**, 4624–4630.

21 M. Irie, *Chem. Rev.*, 2000, **100**, 1685–1716.

22 K. Uno, H. Niikura, M. Morimoto, Y. Ishibashi, H. Miyasaka and M. Irie, *J. Am. Chem. Soc.*, 2011, **133**, 13558–13564.

23 M. Irie, T. Fukaminato, K. Matsuda and S. Kobatake, *Chem. Rev.*, 2014, **114**, 12174–12277.

24 Y. Ooyama, R. Asada, S. Inoue, K. Komaguchi, I. Imae and Y. Harima, *New J. Chem.*, 2009, **33**, 2311–2316.

25 Y. Ooyama, K. Kushimoto, Y. Oda, D. Tokita, N. Yamaguchi, S. Inoue, T. Nagano, Y. Harima and J. Ohshita, *Tetrahedron*, 2012, **68**, 8577–8580.

26 Y. Ooyama, Y. Oda, T. Mizumo and J. Ohshita, *Tetrahedron*, 2013, **69**, 1755–1760.

27 T.-A. Yamagishi, M. Nomoto, S. Ito, S.-i. Ishida and Y. Nakamoto, *Polym. Bull.*, 1994, **32**, 501–507.

28 T.-A. Yamagishi, M. Inowaki, M. Ozawa, Y. Nakamoto, S. Ishida and M. Nomoto, *Kobunshi Ronbunshu*, 2000, **57**, 830–835.

29 H. Matter, M. Nazare, S. Gussregen, D. W. Will, H. Schreuder, A. Bauer, M. Urmann, K. Ritter, M. Wagner and V. Wehner, *Angew. Chem., Int. Ed.*, 2009, **48**, 2911–2916.

30 H. G. Wallnoefer, T. Fox, K. R. Liedl and C. S. Tautermann, *Phys. Chem. Chem. Phys.*, 2010, **12**, 14941–14949.

31 I. S. Youn, D. Y. Kim, W. J. Cho, J. M. Madridejos, H. M. Lee, M. Kolaski, J. Lee, C. Baig, S. K. Shin, M. Filatov and K. S. Kim, *J. Phys. Chem. A*, 2016, **120**, 9305–9314.

